Superresolving optical system with time multiplexing and computer decoding

Amir Shemer, David Mendlovic, Zeev Zalevsky, Javier Garcia, and Pascuala Garcia Martinez

Objects that have slow temporal variations may be superresolved with two moving masks such as pinhole or grating. The first mask is responsible for encoding the input image, and the second one performs the decoding operation. This approach is efficient for exceeding the resolving capability beyond Abbe's limit of resolution. However, the proposed setup requires two physical gratings that should move in a synchronized manner. We propose what is believed to be a novel configuration in which the second grating responsible for the information decoding is replaced with a detector array and some postprocessing digital procedures. In this way the synchronization problem that exists when two gratings are used is simplified. Experimental results are provided for illustrating the utility of the new approach.

OCIS codes: 100.6640, 100.0100, 070.0070, 110.0110.

1. Introduction

Because of the wave nature of light, every optical system can provide only a limited spatial resolution. In terms of spatial frequencies the imaging lens is band limited and has a cutoff frequency determined by its numerical aperture and by the wavelength. Thus enlarging the aperture improves the spatial resolution of the optical imaging system. However, physical lens enlargement is costly, owing to fabrication requirements. The purpose of the superresolution approaches is to obtain a synthetic enlargement of the aperture without changing the physical dimensions of the lens.

Attempts to obtain effectively larger apertures follow a single principle: They are based on certain *a priori* knowledge regarding the object. Some examples of such knowledge are as follows: The object is time independent,[1–3] polarization independent,[4] or monofrequency (λ independent).[5] Recently these theories have been generalized with the concept of space–bandwidth product.[6,7]

One of the most appealing approaches for achieving resolving power, which exceeds the classical limits, is related to temporally restricted objects and is based on two moving gratings.[2] Figure 1 shows a schematic of the optical configuration. An input beam illuminates the input mask that is assumed to be approximately time independent (a temporally restricted object). Close to the input mask a grating is placed, which moves with a velocity V. In Ref. 2 this grating was a Ronchi grating. This grating is attached to the input transparency and is used to encode the spatial information of the object and to allow for its transmission throughout the limited aperture (placed in the center of the imaging system). At the output plane of this system another identical grating, assuming a magnification factor of -1, is placed. It moves along the opposite direction with the same velocity V, and its role is to decode the information passed throughout the aperture. Finally, relay optics images the output into a detector that also acts as a time integrator. It was shown[2] that this configuration is able to increase significantly the effective aperture of the system. In Ref. 3 two Dammann gratings replaced the Ronchi gratings. Dammann gratings[8,9] are binary phase gratings, that have several diffraction orders of equal intensity, used to replicate images of one input object. Use of those gratings allowed us to obtain undis-

A. Shemer, D. Mendlovic (mend@eng.tau.ac.il), and Z. Zalevsky are with the Department of Physical Electronics, Faculty of Engineering, Tel Aviv University, 69978 Tel Aviv, Israel. J. Garcia and P. Garcia Martinez are with Department d'Optica, Universitat de Valencia, C/Dr. Moliner 50, 46100 Burjuassot, Valencia, Spain.
Received 13 April 1999; revised manuscript received 19 August 1999.
0003-6935/99/357245-07$15.00/0

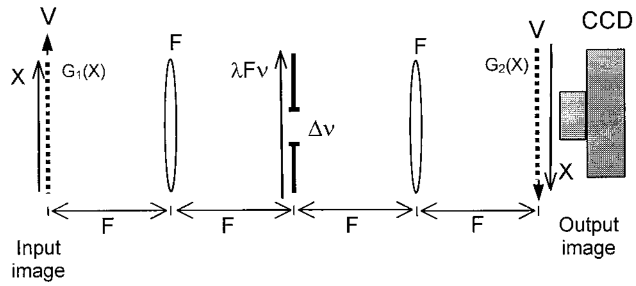

Fig. 1. Optical system for obtaining increased effective aperture with two moving gratings.

torted spatial-frequency transmission of the optical system.

The superresolving approach when two moving gratings are used has two major disadvantages that make it inefficient. One is the need for accurate synchronizing between the gratings. The other is the need for close contact with the gratings in the input and the output planes. In this paper we suggest replacing the second moving grating, which is used for the information decoding, with a virtual grating realized by digital processing with a computer. In this way the synchronization problem that exists when two gratings are used is simplified, and there is no longer a need for attaching the second grating to the output plane.

Section 2 gives a brief explanation for the operation principle of the time-multiplexing approach. Section 3 presents the superresolution when the second grating is removed and produced by a CCD camera and digital processing by computer. Section 4 presents the experimental results.

2. Operation Principle

A hand-waving explanation of the working principle for the conventional system in the coherent case is presented in Fig. 2. Note that the presented explanation is for 3× resolution improvement. The extension for the general case is straightforward. The object's spatial spectrum, $\tilde{U}_0(\nu)$, is divided into sequential spatial-frequency bands defined as

$$a(\nu) = [\tilde{U}_0(\nu)\mathrm{rect}(\nu/\Delta\nu)],$$
$$b(\nu) = [\tilde{U}_0(\nu + v_0)\mathrm{rect}(\nu/\Delta\nu)],$$
$$c(\nu) = [\tilde{U}_0(\nu - v_0)\mathrm{rect}(\nu/\Delta\nu)], \qquad (1)$$

where $\Delta\nu$ is the cutoff frequency of the system and ν_0 is the grating's basic frequency. Thus the overall spatial spectrum can be defined, using the definition of Eq. (1) as

$$\mathrm{FT}[U_0(x)] = \tilde{U}_0(\nu) = [b(\nu)\otimes\delta(\nu+\nu_0) + a(\nu)\otimes\delta(\nu) + c(\nu)\otimes\delta(\nu-\nu_0)], \qquad (2)$$

where $\otimes$ denotes the convolution operation and each band has a bandwidth frequency, which is determined by the aperture diameter. The Fourier transform (FT) of the output intensity distribution equals

$$\tilde{U}_0(\nu) * \tilde{U}_0(\nu) = \left\{\begin{array}{l} [c(\nu) * b(\nu)]\otimes\delta(\nu+2\nu_0) \\ +[a(\nu) * b(\nu) + c(\nu) * a(\nu)]\otimes\delta(\nu+\nu_0) \\ +[a(\nu) * a(\nu) + b(\nu) * b(\nu) + c(\nu) * c(\nu)]\otimes\delta(\nu) \\ +[b(\nu) * a(\nu) + a(\nu) * c(\nu)]\otimes\delta(\nu-\nu_0) \\ +[b(\nu) * c(\nu)]\otimes\delta(\nu-2\nu_0) \end{array}\right\}, \qquad (3)$$

where $*$ denotes the correlation operation. This is the desired output image, which we want to accomplish from the superresolution system. Now, because of the first moving grating, at the spectrum plane of the system each band is encoded with a slightly different wavelength (Doppler effect) [Fig. 2(b)]. It passes through the system with a different (time-dependant) phase that equals $\phi = 2\pi\nu_0 mVt$. This phase multiplies each of the sequential spatial-frequency bands [Fig. 2(c)]. Where ν_0 is the grating's basic frequency, m is the grating's diffraction order and V is the grating's velocity as depicted in Fig. 1. After propagation through the system's finite aperture, which functions as a low-pass filter, a distorted signal is produced [Fig. 2(d)]. At the output plane, decoding (demodulation) is performed with the second moving grating [see Fig. 2(e)]. The output sensing device performs the time-integration operation over the intensity distribution,

$$\frac{1}{\tau}\int_{-\tau/2}^{\tau/2} U_0(x_1, t)U_0^*(x_2, t)\mathrm{d}t. \qquad (4)$$

The integration operation cancels all time-dependant terms that have the form of $\phi = 2\pi\nu_0 mVt$. Hence the following expression is obtained [Fig. 2(e)]:

$$\tilde{U}_1(\nu) * \tilde{U}_1(\nu) = \left\{\begin{array}{l} [c(\nu) * b(\nu)]\otimes\delta(\nu+2\nu_0) \\ +2[a(\nu) * b(\nu) + c(\nu) * a(\nu)]\otimes\delta(\nu+\nu_0) \\ +3[a(\nu) * a(\nu) + b(\nu) * b(\nu) + c(\nu) * c(\nu)]\otimes\delta(\nu) \\ +2[b(\nu) * a(\nu) + a(\nu) * c(\nu)]\otimes\delta(\nu-\nu_0) \\ +[b(\nu) * c(\nu)]\otimes\delta(\nu-2\nu_0) \end{array}\right\}. \qquad (5)$$

Note that Eq. (5) differs from Eq. (3), which is the desired result, by a constant factor generated in each of the frequency bands. Each factor multiplies a different correlated expression, as shown in Fig. 2(f). Each of these correlated expressions can expand up to twice the bandwidth of the optical system. Therefore each band contains terms from bands, which reside next to it, and creates a distortion, which cannot be filtered in the output plane.

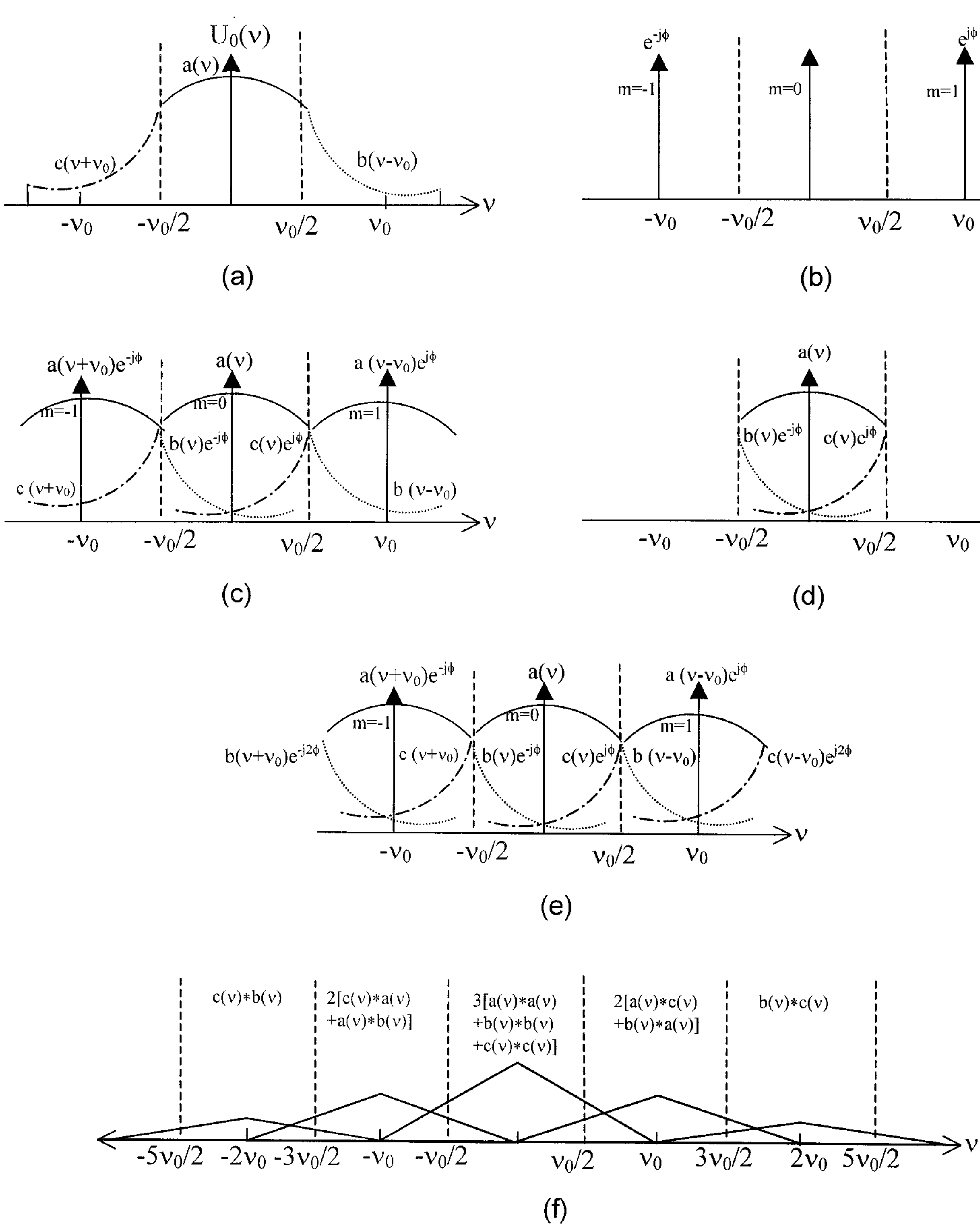

Fig. 2. Superresolution technique in the coherent case: (a) FT of the object, (b) FT of the first moving grating, (c) FT after passing the first grating, (d) FT after passing of the system finite aperture, (e) decoded spectrum after the second grating (same as the first grating) and before time averaging, (f) results after integration by time on the output intensity.

The coefficients of the different terms in Eq. (5) depend on the number of diffraction orders of the grating. For a grating with Q orders, the coefficients will differ starting from Q down to $[Q - (N - 1)]$, where N is the number of spectral bands. Therefore, under the condition that the expanded synthetic aperture is wider than the spectral bandwidth of the input object ($Q \gg N$), a superresolving output is obtained, since Eq. (5) approximates Eq. (3). For example, let us assume that we have a decoding grating that consist of 9 diffraction orders instead of 3 and that the desired enlarged aperture is determined to be three times the effective aperture (e.g., $3\Delta\nu$). After time integration of the intensity distribution, the constant factors of each band change and become 9 for the zero-order band,

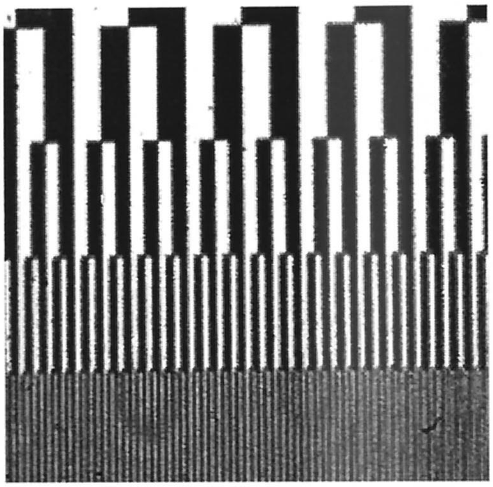

(a)

(b)

Fig. 3. Objects used for the superresolution experiment: (a) grating with a basic period of 125 μm, (b) image of a digital bird (contains information in both axes).

8 for the −1, 1-order bands, and 7 for the −2, 2-order bands, as follows:

$$\tilde{U}_1(\nu) * \tilde{U}_1(\nu) = \left\{ \begin{array}{l} 7[c(\nu) * b(\nu)] \otimes \delta(\nu + 2\nu_0) \\ + 8[a(\nu) * b(\nu) + c(\nu) * a(\nu)] \otimes \delta(\nu + \nu_0) \\ + 9[a(\nu) * a(\nu) + b(\nu) * b(\nu) + c(\nu) * c(\nu)] \otimes \delta(\nu) \\ + 8[b(\nu) * a(\nu) + a(\nu) * c(\nu)] \otimes \delta(\nu - \nu_0) \\ + 7[b(\nu) * c(\nu)] \otimes \delta(\nu - 2\nu_0) \end{array} \right\}. \quad (6)$$

Obviously, this result is a less-distorted spectrum compared with the spectrum achieved when a three-order grating is used.

In a similar way the noncoherent case can also be explained. In this case the input field distribution should have the notation of $U_0(x, t)$, satisfying

$$\frac{1}{\tau}\int_{-\tau/2}^{\tau/2} U_0(x_1, t)U_0^*(x_2, t)\mathrm{d}t = |U_0(x_1)|^2\delta(x_1 - x_2). \quad (7)$$

This results in an enlarged effective aperture, which is obtained without additional approximations. One should note that, owing to the use of Ronchi gratings, different frequency bands pass the system with different strengths. This, of course, distorts the output, mainly by providing a low-pass enhancement. An improvement of the Lukosz basic setup was made by utilization of Dammann gratings[3] instead of Ronchi gratings. These gratings overcome the distortion described above.

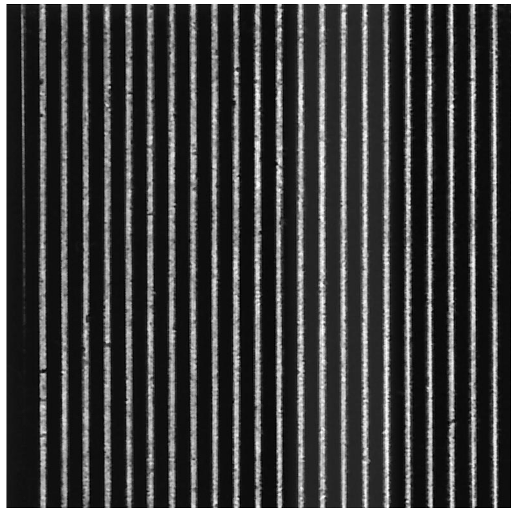

Fig. 4. Ronchi grating used in the setup with a basic period of 125 μm.

3. Superresolution by Computer Decoding

As mentioned above, the main problem with the time-multiplexing superresolution techniques is achieving sufficient synchronization between the two moving gratings. The lack of synchronization causes phase defects in the system's transfer function. Despite the fact that the synchronization problem may be overcome by folding of the optical setup as was done in Ref. 3, one may obtain a more elegant solution at the cost of some digital computation. The first grating attached to the input object will perform the encoding of the input information. Instead of using the second grating, which is supposed to perform the decoding, we will enact decoding by the computer, assuming that $u_0(x, y, t)$ is the field distribution, obtained in the output plane when no decoding grating is used. With an explanation similar to that given in Section 2 but with two-dimensional representation, one determines that

$$G(x, y) = \sum_{n_x}\sum_{n_y} A_{n_x,n_y} \exp[2\pi j(\nu_{0_x}x + \nu_{0_y}y)] \quad (8)$$

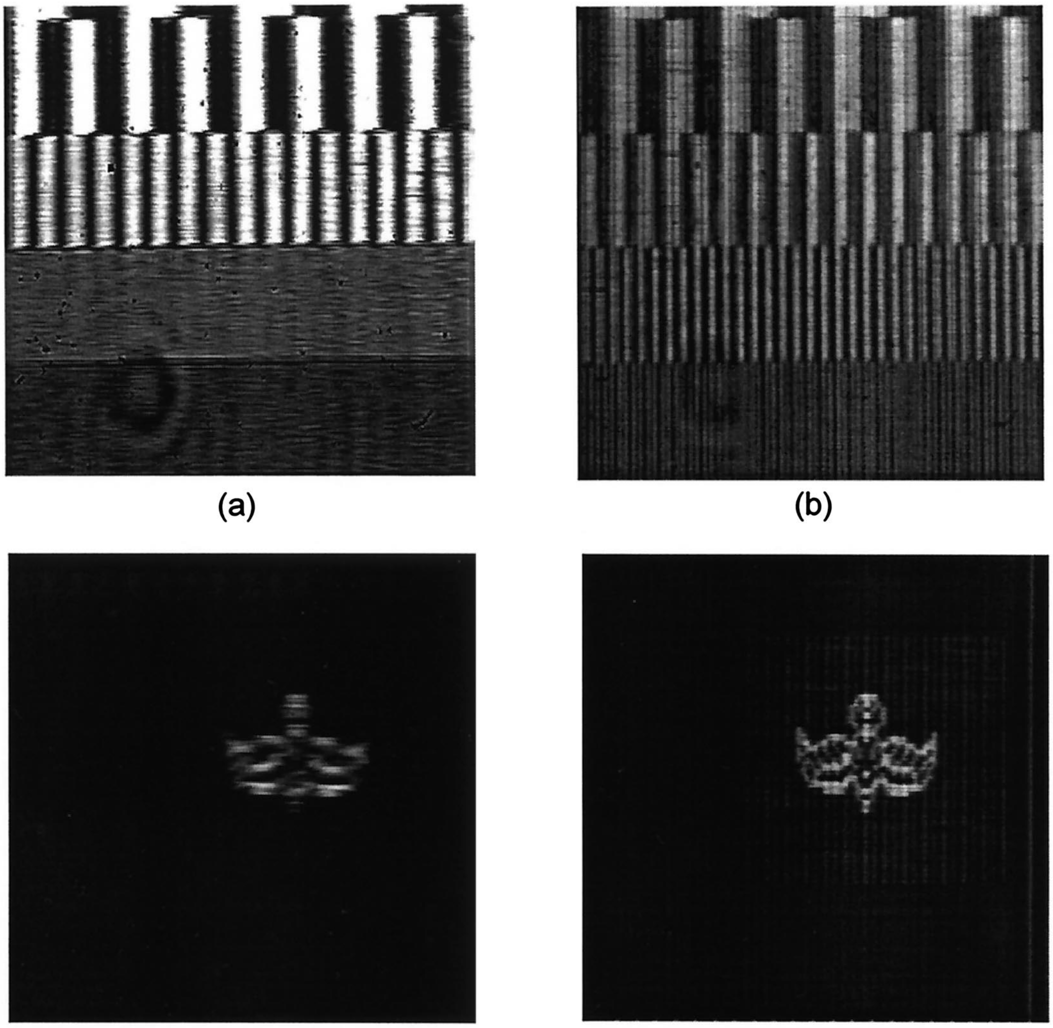

(a) (b) (c) (d)

Fig. 5. Computer-decoding superresolution approach under coherent illumination. With Fig. 3(a) as an object: (a) obtained output without use of the superresolution approach, (b) obtained output with the superresolution approach. With Fig. 3(b) as an object: (c) obtained output without use of the superresolution approach, (d) obtained output with the superresolution approach.

serves as the encoding grating. Note that ν_{0_x}, ν_{0_y} are the basic spatial frequencies of the grating in the x and the y axes, respectively. The instant intensity observed by the CCD camera is

$$I(x, y, t) = u_0(x, y, t)u_0(x, y, t)^*. \tag{9}$$

To obtain superresolution one needs

$$\nu_{0_x} = \Delta\nu_x,$$
$$\nu_{0_y} = \Delta\nu_y, \tag{10}$$

where $\Delta\nu_x$ and $\Delta\nu_y$ are the dimensions of the aperture of the imaging lens in the x and y axes, respectively. Provided that the integration time of the camera is much smaller as compared with $\tau = 1/V\nu_0$, where V is the movement velocity of the grating and ν_0 is its basic spatial frequency (in the corresponding axis), we may assume that the intensity $I(x, y, t)$ is sampled at specific instances of time. According to the mathematical analysis shown in Refs. 3 and 10 it is evident that the multiplication of $u(x, y, t)$ by a second moving grating $G(x - V_x t, y - V_y t)$ and time integration of long period yields the desired result. Note that V_x and V_y are the velocities of the encoding grating along the x and the y axes, respectively. If the decoding grating exists, it should be attached to the output plane, and thus one may write

$$I(x, y) = \frac{1}{\tau}\int_{-\tau/2}^{\tau/2} I(x, y, t)G(x - V_x t, y - V_y t)|^2 \mathrm{d}t, \tag{11}$$

where $I(x, y)$ is the desired superresolved output intensity. Thus, when the decoding grating is missing, the computer will use a series of instantaneous intensities as follows:

$$I_c(x, y) = \sum_{k=1}^{M} I(x, y, t_k)G(x - V_x t_k, y - V_y t_k)|^2, \tag{12}$$

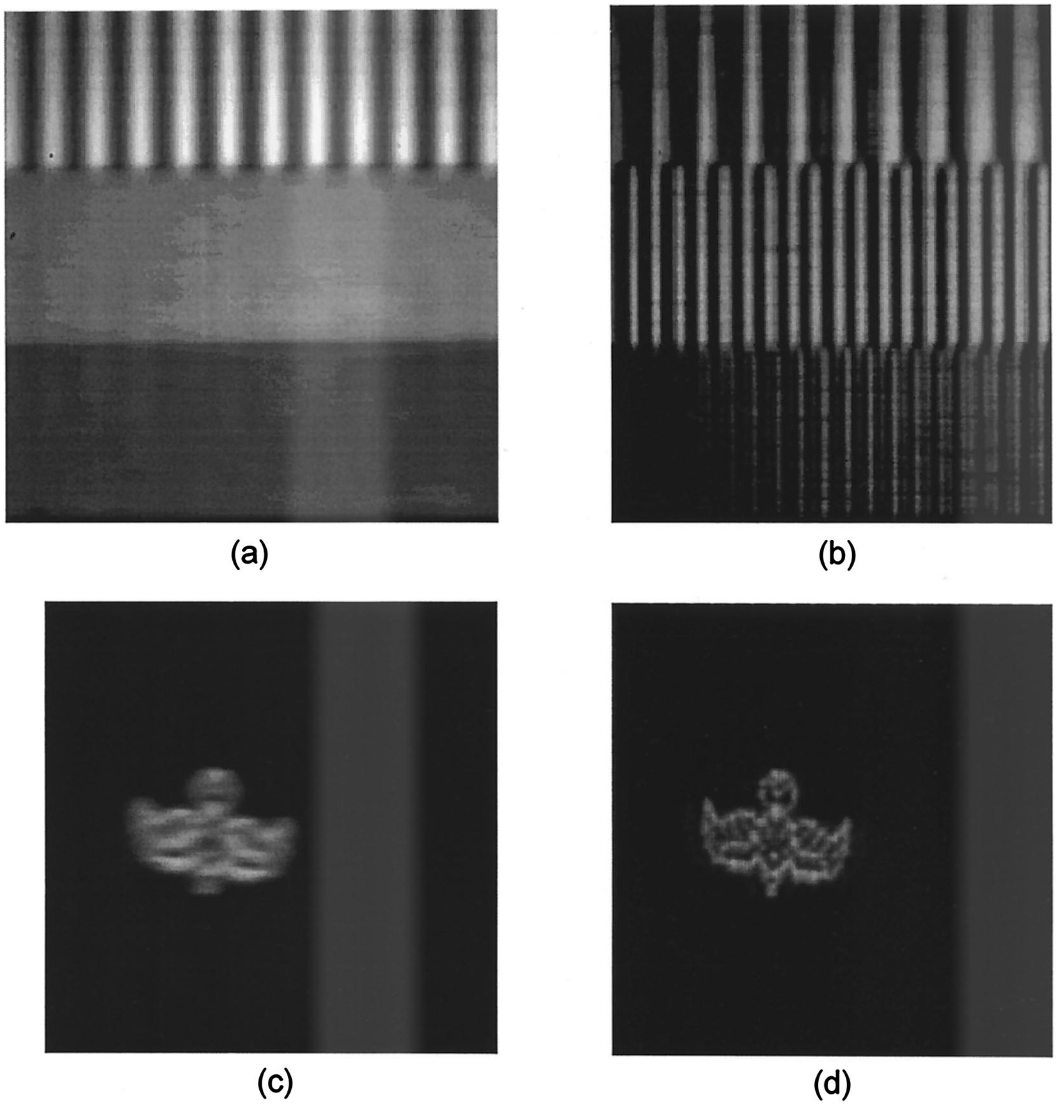

Fig. 6. Same as in Fig. 5 but under noncoherent illumination.

where $I_c(x, y)$ is the intensity obtained after the computer's decoding procedure. For large values of M one will obtain $I_c(x, y) \rightarrow I(x, y)$.

It is important to note that, in comparison with the configurations previously presented, the proposed technique gains three significant advantages: synchronization simplification, processing flexibility, and independence of fabrication defects. The synchronization problem between the computer and the moving grating may be significantly resolved by a digital algorithm. The algorithm will extract (before introduction of the input image) the relative shift phase out of the captured images of the grating, by use of a simple registration technique. The processing flexibility obtained due to the computer may allow us to apply various image-enhancement and image-filtering operations. Since the second grating is generated by the computer, according to the captured images of the first grating, both gratings applied are matched. When two different physical gratings are used, the fabrication defects may create an undesired mismatching that results from reconstruction imperfections.

4. Experimental Results

To demonstrate the suggested approach, experiments were performed for both coherent and noncoherent illuminations. For both illuminations, two types of input were used as seen in Fig. 3. A He–Ne laser of 30 mw and with a wavelength of 632.8 nm was used for the coherent case. For the noncoherent case a white-light halogen lamp was used. The setup for the experiment is the same as in Fig. 1 but without the second grating. The first grating for encoding was a Ronchi grating with a basic period of 125 μm (see Fig. 4). This grating was moved a distance equal to a known fraction of the period, and then the image was grabbed and multiplied with a shifted version of the grating in the computer (the shift in the computer was made according to the shift of the first grating).

A slit with a width of 125 μm was placed in the

Fourier plane (the aperture plane) to mimic a low-performance imaging system. After the Fourier coefficients of the Ronchi grating are exploited, superresolution improvement of at least 3× is anticipated. Figures 5(a) and 5(b) present the obtained output for the coherent illumination when the input of Fig. 3(a) was used. Figure 5(a) is without decoding, and Fig. 5(b) is the image when the computer decoding superresolution approach is used. Figures 5(c) and 5(d) present the same outputs for the input of Fig. 3(b). As one may see, an impressive superresolution effect was obtained. Figure 6 presents the same results as Fig. 5; however, this time a noncoherent illumination was used (the same grating was applied). Here again, the superresolution improvements are easily recognizable.

5. Conclusions

In this paper an approach, believed to be novel, for obtaining time-multiplexing superresolution with computer decoding has been introduced and experimentally demonstrated. The experimental results were obtained for both coherent and noncoherent illumination. The synchronization problem in the former setup, which was the reason for the proposed system, is simplified. In addition, the suggested approach gains the advantages of increasing the processing flexibility and of being independent of fabrication defects. The resulting trade-off is the need for computer calculations, which does not play an essential role in an era of increased digital capabilities.

The obtained experimental results show the optoelectronic capabilities of the proposed optical system. The coherent illumination, although theoretically approximated, shows good results as well.

References

1. M. Francon, "Amélioration de résolution d'optique," Nouvo Climento Suppl. **9,** 283–290 (1952).
2. W. Lukosz, "Optical systems with resolving powers exceeding the classical limit. II," J. Opt. Soc. Am. **57,** 932–941 (1967).
3. D. Mendlovic, A. W. Lohmann, N. Konforti, I. Kiryuschev, and Z. Zalevsky, "One-dimensional superresolution optical system for temporally restricted objects," Appl. Opt. **36,** 2353–2359 (1997).
4. A. W. Lohmann and D. P. Paris, "Superresolution for nonbirefringent objects," Appl. Opt. **3,** 1037–1043 (1964).
5. A. I. Kartashev, "Optical systems with enhanced resolving power," Opt. Spectra **9,** 204–206 (1960).
6. A. W. Lohmann, R. Dorsch, D. Mendlovic, Z. Zalevsky, and C. Ferreira, "Space–bandwidth product of optical signals and systems," J. Opt. Soc. Am. A **13,** 470–473 (1996).
7. D. Mendlovic and A. W. Lohmann, "Space–bandwidth product and its application to superresolution: fundamentals," J. Opt. Soc. Am. A **14,** 558–562 (1997); D. Mendlovic, A. W. Lohmann, and Z. Zalevsky, "Space–bandwidth product adaptation and its application to superresolution: examples," J. Opt. Soc. Am. A **14,** 563–567 (1997).
8. H. Dammann and E. Klotz, "Coherent optical generation and inspection of two dimensional periodic structures," Opt. Acta. **24,** 505–515 (1977).
9. H. Dammann and K. Görtler, "High-efficiency in-line multiple imaging by means of multiple phase holograms," Opt. Commun. **3,** 312–315 (1971).
10. D. Mendlovic, D. Farkas, Z. Zalevsky, and A. W. Lohmann, "High-frequency enhancement by an optical system superresolution for of temporally restricted objects," Opt. Lett. **23,** 801–803 (1998).